

MULTISCALE ANALYSIS OF FORCED AND NATURAL CONVECTION INCLUDING HEAT TRANSFER PHENOMENA IN THE TALL-3D EXPERIMENTAL FACILITY

A. Papukchiev

Gesellschaft fuer Anlagen- und Reaktorsicherheit (GRS) gGmbH
Boltzmannstr. 14, Garching, Germany
angel.papukchiev@grs.de

C. Geffray

Lehrstuhl fuer Nukleartechnik
Technische Universitaet Muenchen
Boltzmannstr. 15, Garching, Germany
clotaire.geffray@ntech.mw.tum.de

M. Jeltsov, K. Kööp, P. Kudinov, D. Grischenko

Division of Nuclear Power Safety
KTH Royal Institute of Technology
Roslagstullsbacken 21, Stockholm, Sweden
marti@safety.sci.kth.se; kaspar@safety.sci.kth.se;
pavel@safety.sci.kth.se; dmitry@safety.sci.kth.se;

ABSTRACT

Within the European FP7 project THINS (Thermal Hydraulics of Innovative Nuclear Systems), numerical tools for the simulation of the thermal-hydraulics of next generation reactor systems were developed, applied and validated for innovative coolants. The Gesellschaft fuer Anlagen- und Reaktorsicherheit (GRS) gGmbH, the Technische Universitaet Muenchen (TUM) and the Royal Institute of Technology (KTH) participated in THINS activities related to the development and validation of computational fluid dynamics (CFD), System Thermal Hydraulics (STH) and coupled STH – CFD codes. High quality measurements from the experiments performed at the TALL-3D facility, operated by KTH, were used to assess the numerical results. This paper summarizes the work accomplished for the validation of the coupled codes ATHLET-ANSYS CFX and RELAP5/STAR CCM+ and highlights the main results achieved for the T01.09 experiment.

KEYWORDS

Innovative reactors, coupled codes, validation

1. INTRODUCTION

STH codes have been developed and applied in the last 35 years to model the behavior of nuclear power reactors. These are based on 1D modeling approaches and therefore are not always capable to predict transients and accidents with pronounced 3D phenomena such as flow mixing or stratification. Initiatives in the nuclear community promote the utilization of CFD programs for the evaluation of reactor safety issues, where the traditional analysis tools show deficiencies. The CFD codes were developed to provide accurate and detailed solution of the fluid flow in three dimensions, but the representation of a complete reactor cooling circuit is still impractical due to the very high computational time. Therefore, STH and CFD codes are coupled to provide a computationally affordable and accurate numerical solution for the simulation of nuclear reactor transients and accidents.

Within the European FP7 project THINS, STH, CFD and coupled 1D-3D thermal-hydraulic (TH) simulations are being carried out for Generation IV nuclear systems. Such facilities utilize innovative fluids, which have different properties and behavior from the ones used in the current nuclear facilities. Approaches for the coupling of the system codes ATHLET and RELAP5 with the 3D CFD programs ANSYS CFX and STAR CCM+ are developed and implemented by GRS and KTH. In order to validate the coupled 1D-3D tools, dedicated experiments with lead-bismuth eutectic (LBE) coolant were performed in Sweden [1]. In one of the specified experiments, T01.09, the primary circuit circulation pump is tripped. This leads to a TH transient in the facility with local 3D phenomena such as mixing and stratification which affect the overall behavior of the cooling circuit. The objective of this paper is to briefly expose the main outcome of the ATHLET-ANSYS CFX and RELAP5-STAR CCM+ validation. Information on the coupling approaches has already been reported in [2,3].

2. TALL-3D EXPERIMENT AND MODEL DEVELOPMENT

2.1. TALL-3D Facility and T01.09 Experiment

The TALL-3D thermal hydraulic loop is an integral 7 m high experimental facility, operated by KTH [1]. It consists of two fully instrumented circuits. The primary circuit consists of three vertical legs, filled with LBE (Fig. 1, left; arrows show flow direction). In the middle leg, a 3D test section is installed (see Fig. 1, center), which is domain of complex 3D effects and source for challenging TH feedback to the rest of the loop. A heater is wrapped around the upper part of the outer test section wall. This enhances the buoyancy effects in the test section at natural circulation conditions. Inside the test section pool, a metal plate prevents the cold LBE from leaving the vessel without extensive mixing with the heated fluid inside it. In the lower part of the left primary leg (called “main heater (MH) leg”) a heated pin is directly immersed in the pipe. The heat exchanger (HX) is installed in the upper part of the right leg, called “heat exchanger leg”. It transfers the heat produced in the primary circuit to the secondary, oil-cooled side.

In one of the specified experiments, T01.09, the main circulation pump is tripped. This leads to a dynamic TH transient in the facility with local 3D phenomena like LBE mixing and stratification which affect the overall loop behavior. T01.09 starts from a steady state forced convection with 1.64 kg/s LBE mass flow rate in the 3D test section leg and 4810 W power in the heater. When the pump is tripped, the mass flow rate in the 3D-leg decreases abruptly and even reverses for a short time. In all following figures the pump is tripped at 0 s. The main boundary conditions are summarized in Table I.

Table I. T01.09 Initial and Boundary Conditions

Parameter	Value/State
Initiation of the pump trip (simulation time)	0 s
Main and 3D test section heaters	always ON
Main heater power	2578 W
3D heater power	4810 W
Mass flow rate in the heat exchanger leg	4.27 kg/s
Mass flow rate in the 3D leg	1.64 kg/s
Mass flow rate in the main heater leg	2.63 kg/s
LBE temperature at the 3D test section and main heater inlet	239 °C
Oil temperature at the inlet of the heat exchanger secondary side	61 °C

The TALL-3D facility is well instrumented with thermocouples (TCs). Only in the test section there are more than 140 TCs. Figure 1 (right) shows the location of the main TC groups in the test section: CIP (circular inner plate TCs), BP (bottom plate TCs), IPT (inner pipe TCs), ILW (inner lateral wall TCs), OLW (outer lateral wall TCs). Each TC group can be found four times in the cylindrical pool – at 0°, 90°, 270° and 360°. Since T01.09 is a symmetric test, the average data of each 4 TCs is compared with the prediction of the simulations.

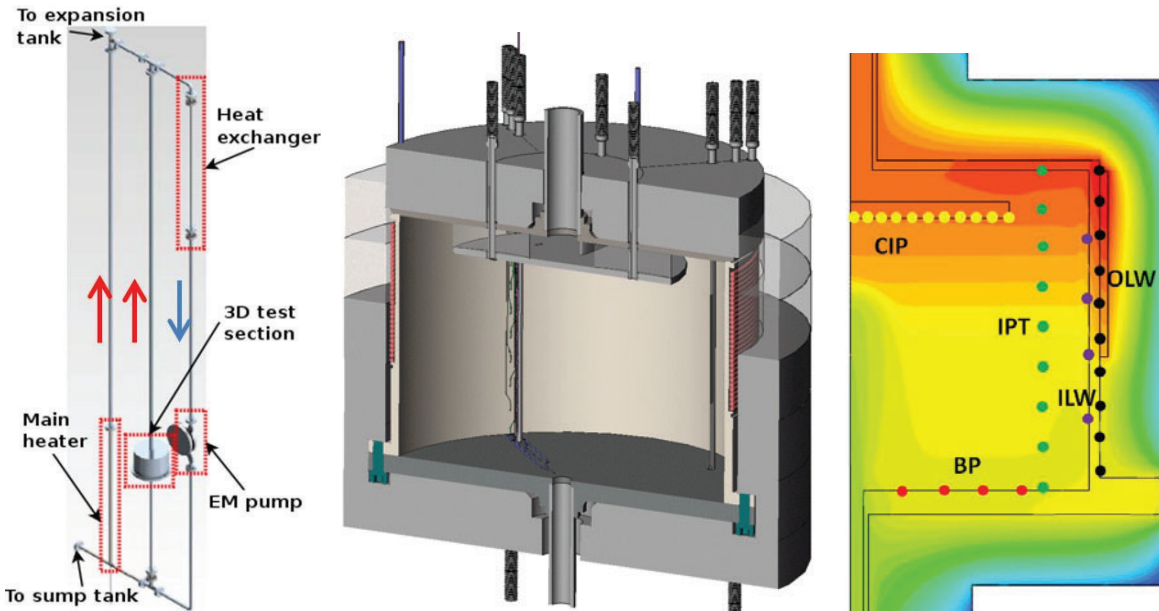


Figure 1. TALL-3D Primary Circuit (left), Test Section (center) and Position of the TC Groups (right).

2.2. Modeling of the TALL-3D Facility with ATHLET-ANSYS CFX and RELAP5-STAR CCM+

Since the TALL-3D experiments are long transients and therefore require substantial computational effort, a 2D model was generated, representing 1° rotational symmetry sector of the test section. This mesh was systematically refined and grid sensitivity studies were performed according to the OECD Best Practice Guidelines [4]. The selected mesh for the final 1° simulations has 109.000 elements (Fig. 2b). The ATHLET-ANSYS CFX calculation presented here was performed with the SST turbulence model [5]. At the test section inlet, 10 % turbulence intensity was specified.

Four priority chains (flow paths) were used for the simulation of the experimental facility with ATHLET. Pressure control is performed with the help of a time dependent volume, which simulates the TALL-3D expansion tank. The secondary circuit is modeled in a simplified way with three pipes. Mass flow rate and enthalpy are specified at the inlet pipe with the help of a FILL component, and the circuit ends with a time dependent volume. The glycerol Dowtherm RP oil used during the experiments at the secondary side of the facility is not available as a fluid in ATHLET or RELAP5. Therefore, the secondary ATHLET circuit was filled with water. Since the oil mass flow rate in the secondary side has been kept constant during the TALL-3D T01.09 experiment, temperature dependent wall-oil heat transfer coefficient (HTC) using Sieder and Tate correlation was calculated [6]. ATHLET allows the user to specify a HTC in the input deck and to utilize it during the calculation. The insulation of the facility is modeled with heat conduction objects (HCOs) with material properties such as heat conductivity, heat capacity, density. In

addition, the heat transfer between the insulation outer wall and the surrounding air is modeled with specified HTC. The whole facility model comprises approx. 170 control volumes (Fig. 2a). For the ATHLET-ANSYS CFX simulations an adaptive time stepping scheme (time step sizes between 0.05 and 0.1 s) was selected.

The 2D axisymmetric mesh for STAR CCM+ consists of 14.800 polyhedral cells (Fig. 2c). The outlet and inlet pipes are modeled with 25 prism layers and the rest of the domain is modeled with 15 layers on the wall [7]. For transient simulations, unsteady implicit time integration scheme is used with second order temporal discretization. Segregated solver with second order upwind convection scheme is selected for the flow [8]. Mixed convection turbulence inside the 3D test section is predicted using a Realizable K-Epsilon turbulence model with Buoyancy Driven Two Layer formulation developed by Xu et al. [9].

The corresponding RELAP5 nodalization of TALL-3D geometry can be seen in Fig. 2d. The model consists of pipe structures connected together by single junctions and time-dependent junctions. Time-dependent volumes are used for the expansion tank and the secondary side inlet and outlet.

The main differences related to the modeling in ATHLET and RELAP5 are related to the LBE properties, heat transfer correlations, and the trip of the pump. In ATHLET and ANSYS CFX the OECD/NEA LBE properties are implemented [10], while RELAP5 relies on Sobolev data [11]. TUM compared both data and found that the differences between these two packages were not significant. For the calculation of the Nusselt number in ATHLET the Cheng and Tak correlation [12] is used. In RELAP5, the Seban-Shimazaki correlation is applied. The electromagnetic pump is modeled in RELAP5 with a time-dependent junction with a bypass for natural circulation. This means that at forced flow conditions the model has a predefined mass flow rate through the HX leg. When the pump is tripped, the flow is only defined by the pressure balance in the primary loop. In ATHLET input deck the pump is modeled, whereas the pump differential pressure is controlled by a signal. The signal is deactivated when the pump is tripped.

The main objective of this work was to validate ATHLET-ANSYS CFX and RELAP5/STAR CCM+ on experimental data. The 2D CFD modelling approach seems to be adequate, since the flow pattern in this transient is symmetric. Different nodalizations, grids, turbulence models, time step sizes etc were used in the calculations. Both programs rely on different numerical approaches and the parameters for each simulation were selected according the best knowledge and experience at GRS and KTH.

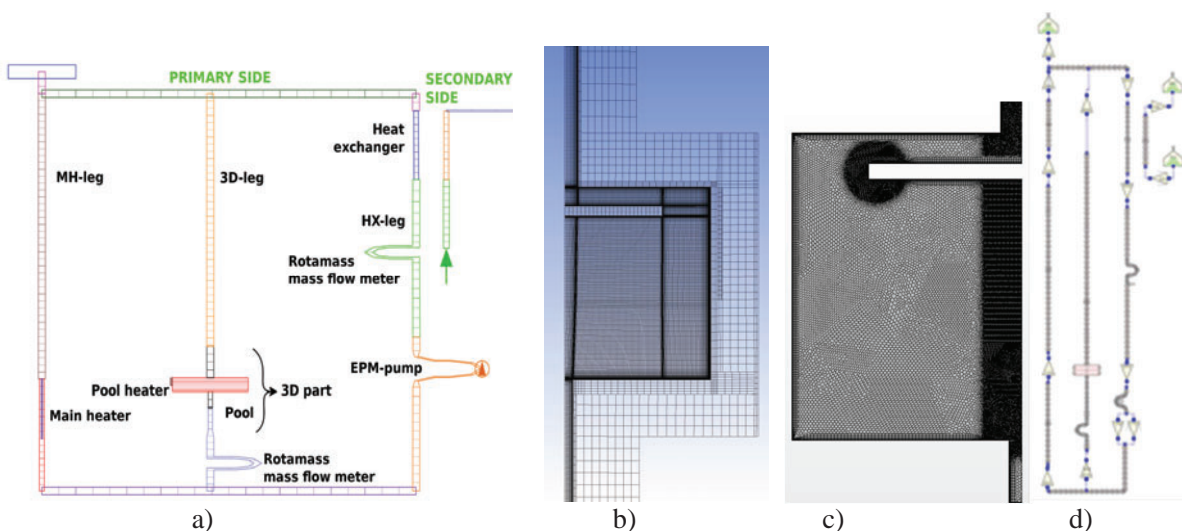


Figure 2. ATHLET (a), ANSYS CFX (b) STAR CCM+ (c) and RELAP5 (d) Models.

3. CODE VALIDATION AND DISCUSSION ON THE TALL-3D RESULTS

In this chapter the transient progression in T01.09 is described. Results from the STH stand-alone and coupled calculations are analyzed and directly compared with measured data. The comparison is first performed for global scale TH parameters in order to evaluate the overall facility behavior. Local scale TH parameters reveal the phenomena occurring inside the 3D test section.

3.1 TH Phenomena and Global Facility Behavior

The simulations begin from a steady state with pump switched on. Three large vortices develop (Fig. 3, left) in the ANSYS CFX domain. The cold LBE first hits the circular inner plate and then moves to the side pool wall, taking the heat away from it and transporting it to the center and the bottom part of the pool. As a result, a mixed flow pattern in the 3D test section pool is observed (see Fig. 3, right). At $t=0$ s the electromagnetic pump is tripped with a run down time of seven seconds, which leads to a rapid mass flow rate decrease in all three primary legs. Within ten seconds the LBE mass flow rate in the HX leg drops from 4.27 kg/s to 0.25 kg/s and then stabilizes at about 0.55 kg/s. Due to the LBE density distribution in the primary circuit and the difference between the geodetic heights of both heaters (lower part of the facility) and the HX (upper part of the facility), natural LBE circulation occurs in the primary circuit of the TALL-3D facility immediately after the pump trip. In this early phase of the transient, a mass flow increase in the MH leg is observed, while the LBE mass flow rate in the 3D test section leg decreases further (Fig. 4). In all calculations, the LBE flow even reverses for approx. 75 s, while in the experiment it is for 100 s. The reason for the reverse flow in the 3D leg is the strong natural circulation in the MH leg. The mass flow rate distribution in both legs is determined in this early transient phase by the volumes of the MH pipe and the test section pool. Since the volume of the MH pipe ($4.92E-4$ m³) is significantly smaller than the one of the 3D test section pool ($141.37E-4$ m³), the LBE is heated more rapidly in the MH (up to 298 °C, see first temperature peaks around $t=75$ s in Fig. 5), and its outlet temperature increases faster than the LBE temperature at the outlet of the test section outlet pipe (Fig. 6). Approximately 170 s later, the flow in the 3D leg increases and hot LBE is transported from the pool to the test section outlet. The temperature peak of 336 °C (Fig. 6) is well captured by all four codes, although ATHLET and RELAP5 predict it slightly earlier in the transient progression.

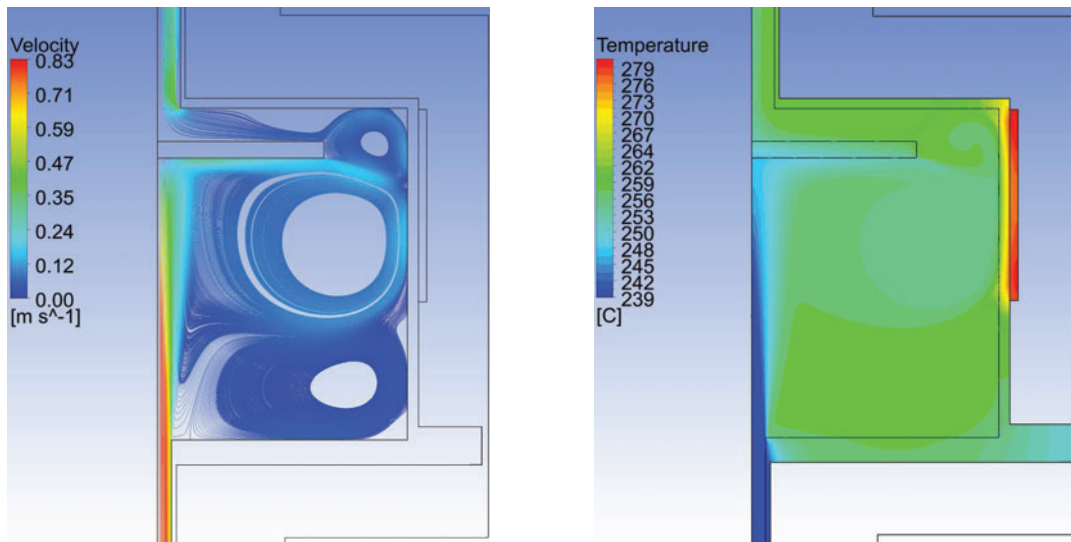


Figure 3. Streamlines Colored with Velocity (left) and Temperature Distribution (right) in the 3D Test Section Pool at Forced Circulation Conditions, Obtained with ANSYS CFX.

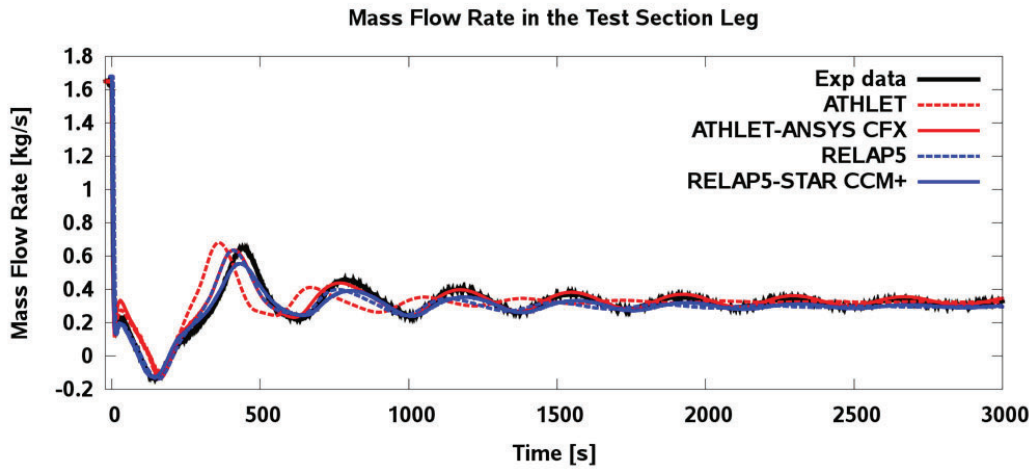


Figure 4. Mass Flow Rate in the 3D Leg.

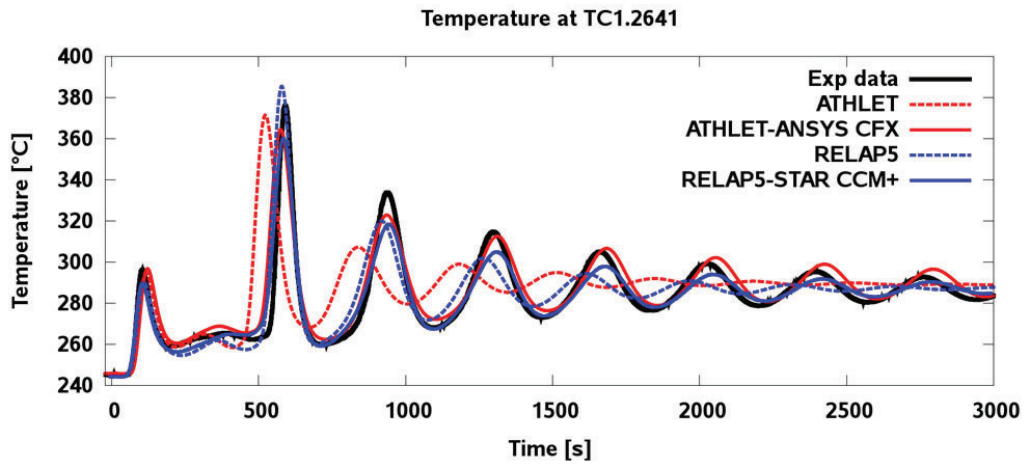


Figure 5. Temperature at the MH Outlet.

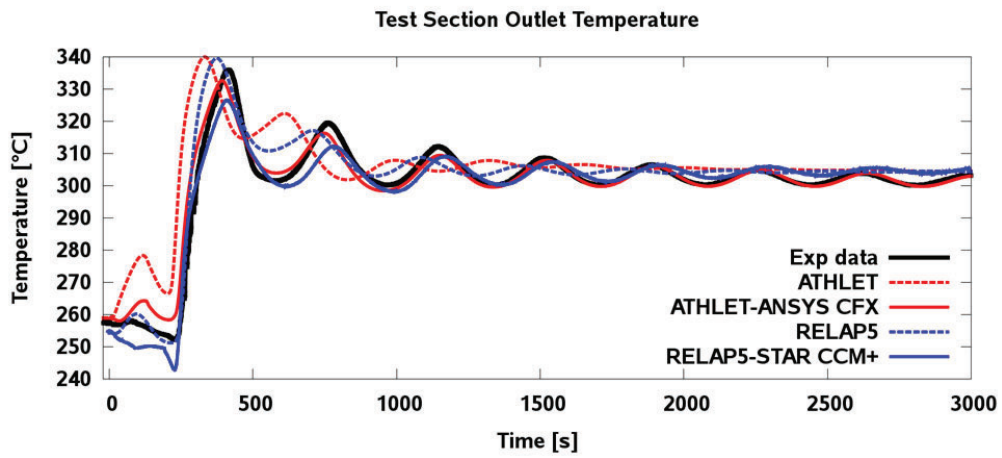


Figure 6. Temperature at the 3D Test Section Outlet.

Figure 7 shows the evolution of the LBE temperature at the inlet of the test section inlet pipe. Approximately 110 s after the initiation of the transient, the measured temperature at the test section inlet (238 °C) suddenly starts to increase and after 40 s reaches 251 °C. This is also observed in both coupled simulations. In ATHLET and RELAP5 calculations this increase is not present. For the forced circulation steady state, a system code like ATHLET or RELAP5 will predict stratification in the test section. This is consequence of the 1D lumped parameter approach implemented in these programs. Since the heater is installed around the upper half of the test section pool wall, only the nodes in this part are actually heated, while the ones below the heater are still filled with cold LBE ($T_{LBE}=T_{inlet}$). In this way, a 1D system code will predict (as expected) stratification in the test section, which does not exist in reality. In the coupled calculation, three large vortices develop in the CFD domain. As a result, a mixed flow pattern in the 3D test section pool is observed and the temperature at the pool bottom is significantly higher compared to the one, observed at the pool inlet (see Fig. 3, right). In flow reverse conditions this hot LBE is transported to the inlet of the test section inlet pipe, as observed in Fig. 7. In case of STH the LBE from the cold lower pool part flows through the test section inlet pipe. The short duration of the flow reversal and the very small velocities ($1.5E-4$ m/s) impede the transport of heated LBE from the upper ATHLET or RELAP5 pool parts to the test section inlet pipes (total flow path ~ 0.6 m). As a consequence, no temperature increase can be observed in the both 1D STH calculations.

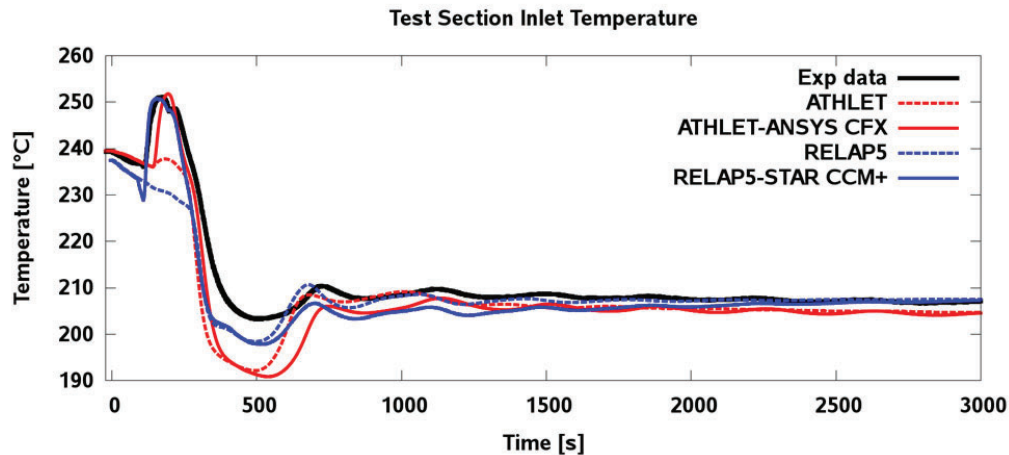


Figure 7. Temperature at the 3D Test Section Inlet.

After the pump trip, the LBE flows slowly through the primary HX tube at natural circulation conditions. It is intensively cooled by the cold secondary side, kept at constant mass flow rate of 0.06 kg/s and at a temperature of 61 °C. The LBE temperature at the outlet of the HX drops from approx. 240 °C down to 186 °C (Fig. 8). After the first low peak, the temperature at the HX outlet (primary side) starts to increase due to the increasing temperatures at the outlets of the test section and MH. A very good prediction is observed in the RELAP5-STAR CCM+ simulation in the first 250 s of the transient, while ATHLET-ANSYS CFX underestimates the LBE temperature by 3 to 5 K.

After the pump trip the LBE in the test section pool starts to heat up. Approximately 250 s after the initiation of the transient the heated, light LBE starts to flow in its normal direction and 100 s later appears at the outlet of the test section (see Fig. 6). The enhanced natural circulation in the 3D leg reduces the LBE flow rate in the MH leg to its minimum value of -0.07 kg/s (flow reversal). The small LBE velocities lead to the heating of the liquid metal in the MH up to 384 °C (Fig. 5). ATHLET-ANSYS CFX and RELAP5-STAR CCM+ underpredict the peak by approx. 10 K, while RELAP5 overpredicts it. The

smallest deviation from data (3 K) is observed in ATHLET calculation, but unfortunately, with some offset in the time.

It can be seen that a very dynamic and oscillatory TH behavior of the primary TALL-3D loop has been achieved by the KTH experimentalists with the selected boundary conditions for T01.09. After 3000 s, the TALL-3D facility reaches a new steady state at natural circulation conditions. Figure 9 shows the temperature distribution in the test section at natural circulation conditions (t=3000 s). The stabilized mass flow rates in the primary side lead to a stable thermal stratification in the pool.

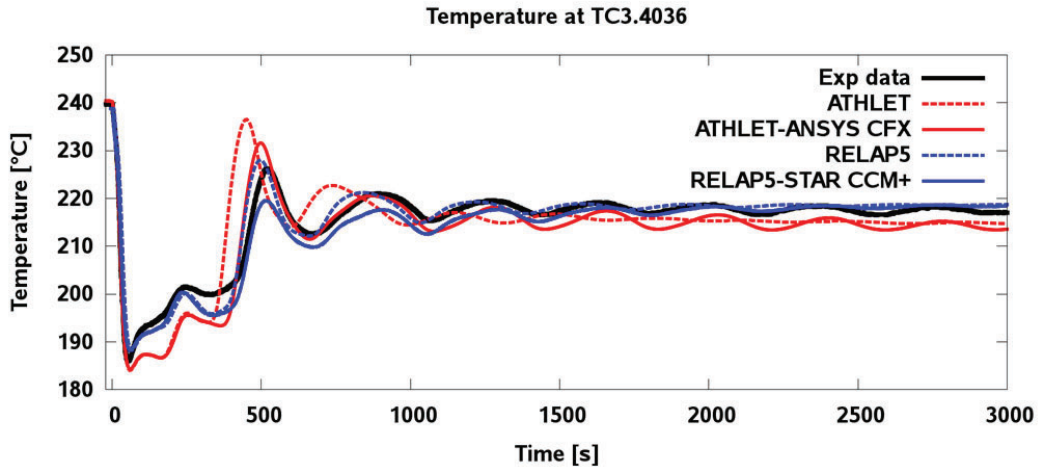


Figure 8. Temperature at the HX Outlet (Primary Side).

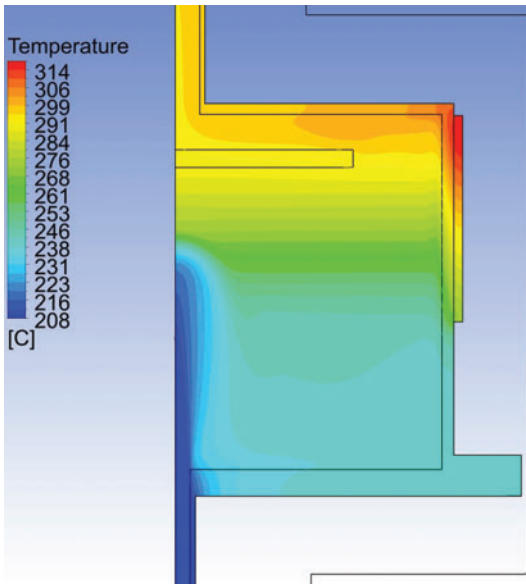


Figure 9. Temperature (natural circulation)

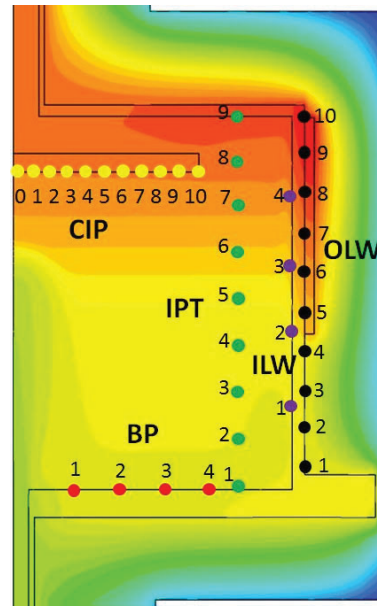


Figure 10. TCs in the Test Section

3.2 Comparison of Local TH Parameters in the Test Section Pool

In this subchapter only ATHLET-ANSYS CFX and RELAP5-STAR CCM+ results from the coupled calculations are presented, since the 1D simulation approaches in ATHLET and RELAP5 cannot provide local temperatures inside the pool. Figure 10 shows the exact position of the TCs, discussed in the following figures.

The comparison for the bottom plate (BP) TCs is shown in Figs. 11 and 12. ATHLET-ANSYS CFX captures very well the first part of the transient, while the temperature is underestimated by up to 8 K over the transient phase 450-2000 s. Thereafter, a good agreement is observed in both figures. RELAP5-STAR CCM+ underestimates the BP temperatures during the transient phase and at steady state forced circulation conditions. Both codes show similar underpredictions also for the inner pipe TCs IPT1 and IPT3 (Figs. 13 and 14), positioned in the lower pool part. ATHLET-ANSYS CFX agrees well with IPT7 and IPT9 data (Fig. 15 and Fig. 16), while RELAP5-STAR CCM+ shows some deviations. The comparison for the inner lateral wall TCs ILW1 and ILW4 is shown in Figs. 17 and 18. Once again the agreement with data is better in the upper pool part. The comparison for the OLW TCs is shown in Figs. 19, 20 and 21. Some inconsistencies, associated with the OLW experimental data in the heater region were discovered. Therefore, only OLW temperatures in the lower pool part are shown.

The circular inner plate (CIP) TCs are positioned on the lower surface of the circular inner plate. CIP0 (Fig. 22) is located over the very center of the plate, while CIP 10 (Fig. 24) is positioned at its outer edge. CIP5 (Fig. 23) is in the middle between CIP0 and CIP10. The low temperature peaks in Fig. 22 appear, because the oscillating cold LBE jet impinges on the plate. The first two CIP0 peaks are simulated very well by the coupled codes, while the next ones are not captured by any calculation. The agreement for CIP5 (Fig. 23) is good, except for the missing first low peak. At CIP10 location, such peak is not present, because it is far away from the front of the LBE jet. One can conclude that the exact shape of the impinging jet is not precisely captured by the calculations. The possible reasons for this are discussed in the next subchapter.

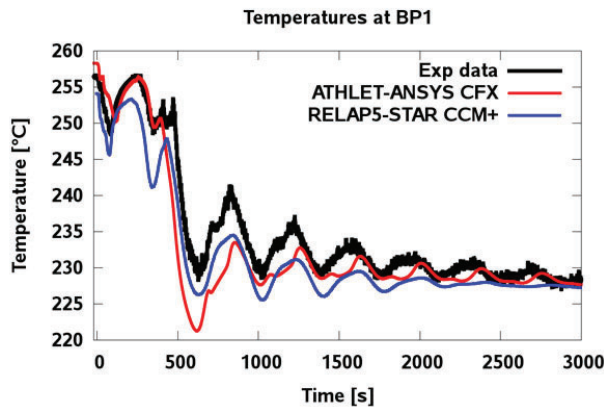


Figure 11. Temperature at BP1.

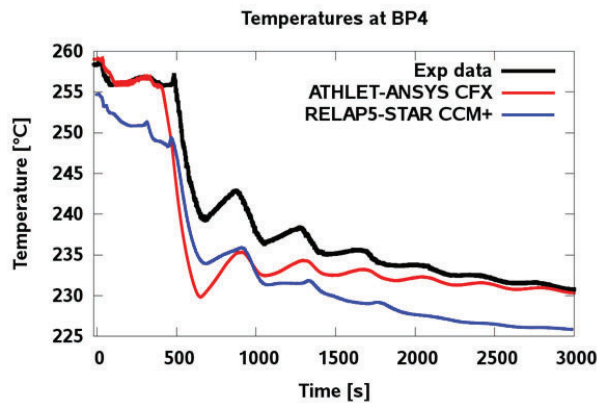


Figure 12. Temperature at BP4.

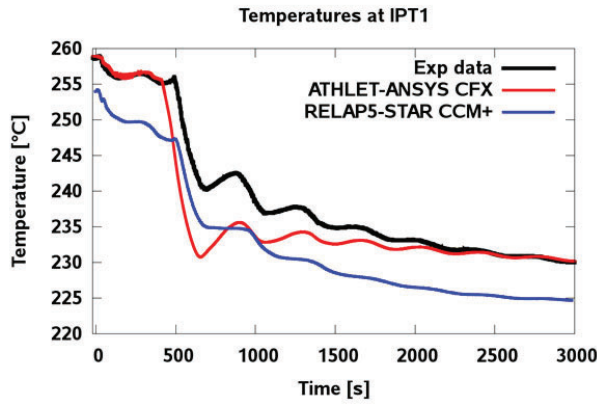


Figure 13. Temperature at IPT1.

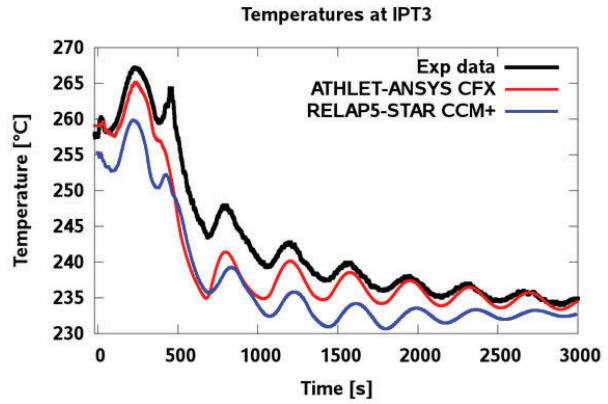


Figure 14. Temperature at IPT3.

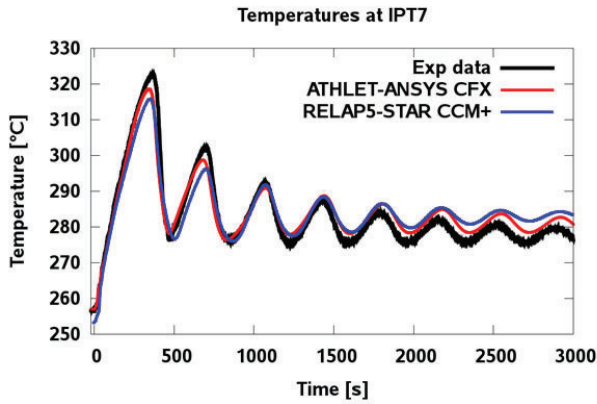


Figure 15. Temperature at IPT7.

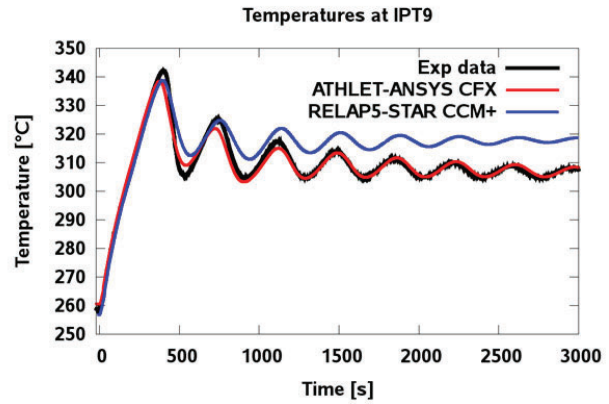


Figure 16. Temperature at IPT9.

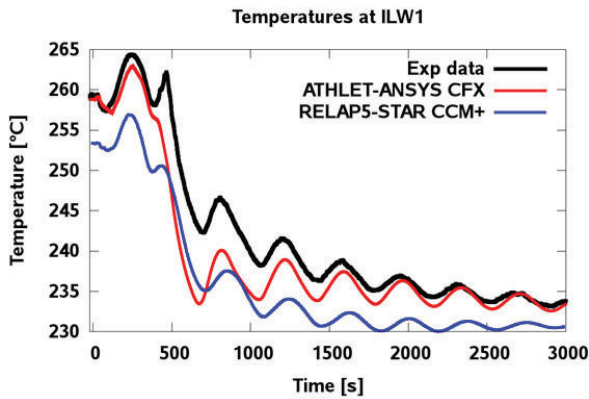


Figure 17. Temperature at ILW1.

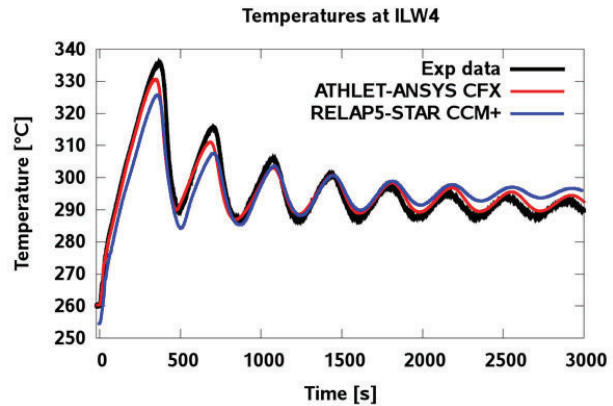


Figure 18. Temperature at ILW4.

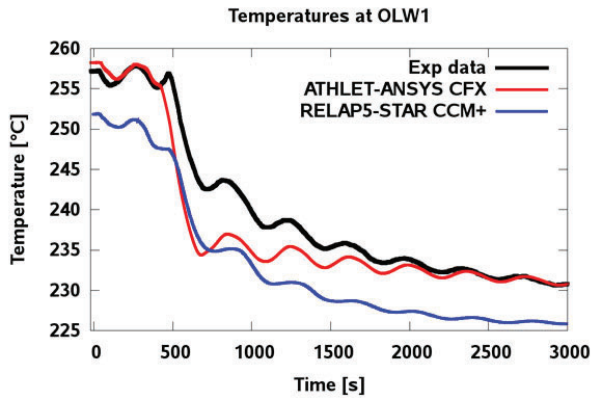


Figure 19. Temperature at OLV1.

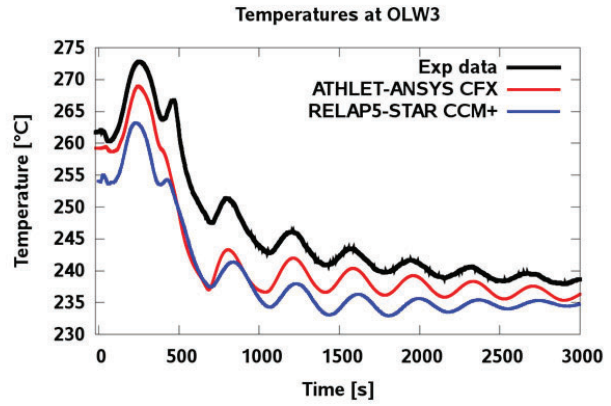


Figure 20. Temperature at OLV3.

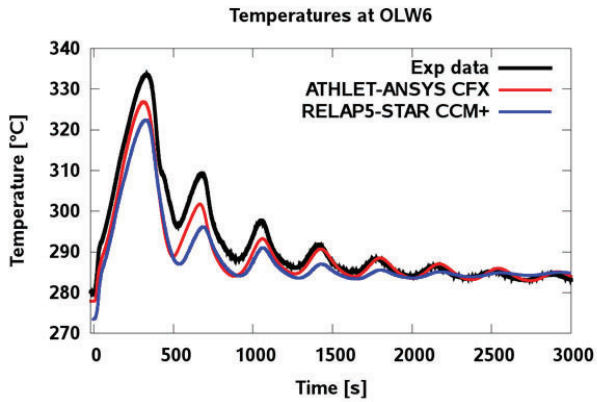


Figure 21. Temperature at OLV6.

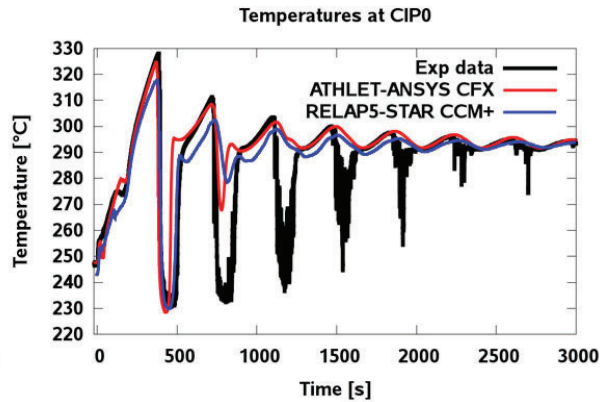


Figure 22. Temperature at CIP0.

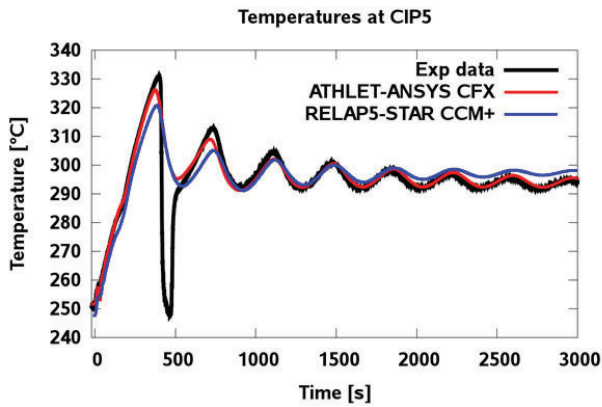


Figure 23. Temperature at CIP5.

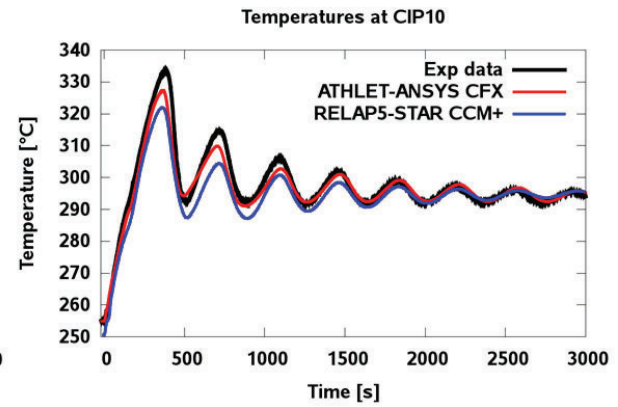


Figure 24. Temperature at CIP10.

3.3 Discussion of the Results

The figures in this section show that all four calculations represent qualitatively well the behavior of the TALL-3D facility. It is also obvious that the coupled codes ATHLET-ANSYS CFX and RELAP5-STAR CCM+ perform better than ATHLET and RELAP5 stand-alone. The STH codes with their simplifications are not capable to capture correctly the transition from forced to natural circulation condition. Complex TH processes in the test section provide important feedback to the rest of the circuit, which has to be considered in the numerical simulation. Without consideration of the 3D flow mixing at forced circulation and stratification at natural circulation in the pool and the transition between these two states, it is hard to achieve good results. In the figures presented in chapter 3.1 it is evident that the details of the loop dynamic behavior are lost in the 1D simulations. Temperature and mass flow oscillations are damped in these calculations very fast (see Fig. 6). This is due to the simplifications in the 1D representation and the larger numerical diffusion.

Concerning the local temperature values inside the test section, larger temperature underestimation in the lower pool part (see BPs, IPT1, ILW1, OLW1 with up to 10 K deviation from experiment) is present between $t=500$ s and $t=1500$ s. The reason for these colder temperatures in ATHLET-ANSYS CFX simulation is related to the colder temperature at the test section inlet between 350 – 700 s (see Fig. 8), which is related to the underestimation of the temperature at the heat exchanger outlet. This leads to the observed temperature underestimation for BPs, IPT1, ILW1, OLW1 TCs in the ATHLET-ANSYS CFX simulation.

In order to better assess the performance of ATHLET-ANSYS CFX in the CFD domain, ANSYS CFX stand-alone simulations were performed. Measured data was imposed at the inlet and the outlet of the domain. The comparison with the experimental data revealed consistent results and very good agreement with the experimental data. This proved the capability of the CFD code to simulate properly T01.09. Small inconsistencies were observed only for the CIPs. However, it is well known, that impinging jets represent a major challenge for the two-equation eddy viscosity turbulence models. Moreover, the 2D mesh represents an additional constraint for its proper simulation. An adequate simulation of the LBE jet requires the utilization of advanced turbulence techniques. Scale resolving simulations (SRS) such as large eddy simulation (LES), zonal large eddy simulation (ZLES) or scale adaptive simulation (SAS) together with 3D CFD meshes (90° or larger symmetry sectors) would be more appropriate for the prediction of flows with impinging jets. More details on the stand-alone ANSYS CFX calculations can be found in [13]

The most challenging part of the T01.09 transient is the transition from forced to natural circulation. In order to predict the temperature distribution in the facility correctly, the mass flow rates in the different legs need to be calculated very accurately. Nonetheless, at mixed and natural convection conditions, this mass flow rate strongly depends on the density, which is directly related to the aforementioned temperature. A direct comparison between ATHLET-ANSYS CFX and ANSYS CFX has been made to show how important the mass flow rate for the results is. The picture on the left side in Fig. 25 represents the temperature distribution in the 3D test section at $t=770$ s (second low temperature peak in Fig. 22) calculated with the coupled code and the picture on the right side the temperature prediction by ANSYS CFX with measured mass flow rate at the inlet. With a mass flow rate in the coupled simulation lower by just 0.03 kg/s from the measured one, the top part of the LBE jet slightly touches the plate (see Fig. 25, left). In the stand-alone ANSYS CFX simulation with the measured mass flow rate the cold core of the jet impinges well on the plate surface (see Fig. 25, right). As a result, the low temperature peaks for CIP0 last longer. These are in better agreement with experimental data (see blue curve in Fig. 26).

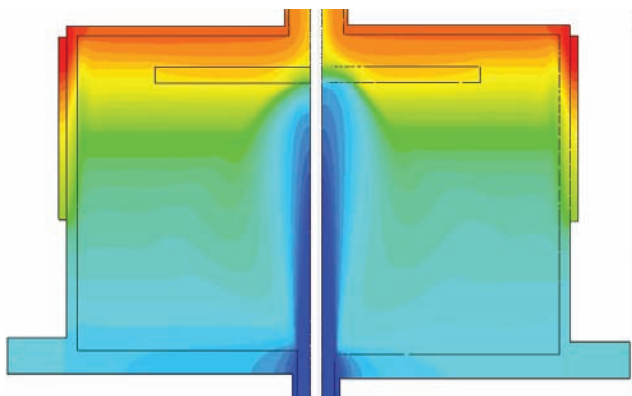


Figure 25. Temperature Distribution in the 3D Pool Calculated by ATHLET-ANSYS CFX (left) and ANSYS CFX (right).

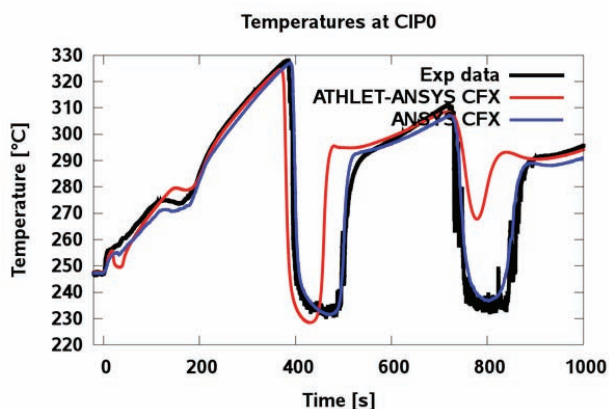


Figure 26. CIP0 Temperature Calculated by ATHLET-ANSYS CFX (calculated mass flow) and ANSYS CFX (measured mass flow).

4. CONCLUSIONS

The performed simulations show that the selected geometry of the TALL-3D facility together with the selected boundary conditions result in a dynamic experiment. This involves complex physics including liquid metal at forced and natural circulation combined with 3D mixing and stratification phenomena and conjugate heat transfer. The configuration with two heaters and one HX in the primary circuit leads to a dynamic mass flow distribution and to a competition between the two heated legs. All four simulations show more or less similar behavior of the main TH parameters. Nevertheless, it was shown, that the 1D models are not always adequate for the simulation of flows with pronounced 3D effects such as mixing and stratification. ATHLET and RELAP5 have difficulties to calculate the correct frequency and amplitude of the mass flow rate and temperature fluctuations in the TALL-3D facility. The main reason for these discrepancies lies in the 3D effects like mixing and stratification, which cannot be captured by 1D code. Such flow phenomena affect the thermal-hydraulics not only in the test section but also in the whole facility. The mass flow and temperature fluctuations are smeared by the 1D lumped parameter approach implemented in ATHLET and RELAP5, while the coupled programs reproduce the transient more realistically. Potential improvements might be achieved with further calibration of the system code input decks (pressure and heat losses), which will provide at the inlets of ANSYS CFX and RELAP5 mass flow rate and temperature values even closer to the experimental ones. This will significantly reduce the observed deviations in section 3.2. The 2D axisymmetric CFD models provided good results for the most of the TCs. One should not forget that T01.09 is a symmetric transient and this approach will not work for asymmetric 3D flows. Moreover, the impinging jet area (CIPs) is not resolved correctly by the CFD codes even in stand-alone mode [13]. Larger TALL-3D models (90° sector or full CFD model) would allow the utilization of advanced turbulence models such as LES, ZLES, SAS, etc.

ACKNOWLEDGMENTS

This work was supported by the EC 7th Framework Project THINS (Thermal-Hydraulics of Innovative Nuclear Systems, Grant No. 249337) and partly financed by the German Federal Ministry for Economic Affairs and Energy.

REFERENCES

1. D. Grishchenko, M. Jeltsov, K. Kööp, A. Karbojian, W. Villanueva and P. Kudinov “The TALL-3D facility design and commissioning tests for validation of coupled STH and CFD codes” Nuclear Engineering and Design, In Press, available online 11 February 2015.
2. A. Papukchiev and G. Lerchl, “Development and Implementation of Different Schemes for the Coupling of the System Code ATHLET with the 3D CFD Program ANSYS CFX”, Proc. of the NUTHOS-8 Conference, Shanghai, China, October 10-14, 2010.
3. M. Jeltsov et al, “Development of a Domain Overlapping Coupling Methodology for STH/CFD Analysis of Heavy Liquid Metal Thermal-hydraulics”, Proc. of the NURETH-15 Conference, Pisa, Italy, May 12-17, 2013.
4. OECD/NEA, "Best Practice Guidelines for the use of CFD in Nuclear Reactor Safety Applications", NEA/CSNI/R(2007)5, 2007.
5. F. Menter, “Two-Equation Eddy-Viscosity Turbulence Models for Engineering Applications”, *AIAA-Journal*, **32**, pp. 269 – 289, 1994.
6. C. Geffray, A. Papukchiev, D. Grishchenko, P. Kudinov and R. Macián-Juan “Development of Multiscale Thermal-Hydraulic Model of the TALL-3D Facility and Validation with Experimental Data”, Proc. of the ICAPP 2015. Conference, Nice, France, May 3-6, 2015, accepted for publication.
7. P. Kudinov, “Synthesis Note on Sub-WP5.2 Activities”, THINS Deliverable D5.2.05, KTH, 2015.
8. CD-Adapco, “Star-CCM+ User Guide version 7.04.011”, 2012.
9. Xu, W. et al, “A New Turbulence Model for Near-Wall Natural Convection”, *Int. J. Heat and Mass Transfer*, **41**, 3161-3176, 1998.
10. OECD/NEA, “Handbook on Lead-Bismuth Eutectic Alloy and Lead Properties, Materials Compatibility, Thermal-Hydraulics and Technologies” NEA No. 6195 (2007).
11. V. Sobolev, “Database of Thermophysical Properties of Liquid Metal Coolants for GENIV,” SCK•CEN-BLG-1069, 2011.
12. X. Cheng, N. Tak, “Investigations on Turbulent Heat Transfer to Lead-bismuth Eutectic Flows in Circular Tubes for Nuclear Applications”; *Nuclear Engineering and Design* **236**, 385-393; 2006
13. A. Papukchiev and S. Buchholz “Validation of ANSYS CFX for Gas and Liquid Metal Flows with Conjugate Heat Transfer within the European Project THINS”, Proc. Of the NURETH-16 Conference, Chicago, USA, August 30, September 4, 2015.